to provide better overwinter conditions for the krill. Salps compete with krill for phytoplankton – in poor sea ice years salp numbers are increased and krill recruitment is reduced. Further north in their range, *E. superba* abundance is dependent on the transport of krill in the ocean currents as well as fluctuations in the strength of particular cohorts.

Given the importance of euphausiids in marine food webs throughout the world's oceans, they are potentially important indicator species for detecting and understanding climate change effects. Changes in ocean circulation or environmental regimes will be reflected in changes in growth, development, recruitment success, and distribution. These effects may be most notable at the extremes of their distribution where any change in the pattern of variation will result in major changes in food web structure. Given their significance as prey to many commercially exploited species, this may also have a major impact on harvesting activities. A greater understanding of the large-scale biology of the euphausiids and the factors generating the observed variability is crucial. Obtaining good long-term and large-scale biological and physical data will be fundamental to this process.

See also

Antarctic Circumpolar Current. Baleen Whales. Copepods. Phalaropes. Plankton. Sea Ice: Overview. Seals. Sperm Whales and Beaked Whales.

Further Reading

Constable AJ, de la Mare W, Agnew DJ, Everson I and Miller D (2000) Managing fisheries to conserve the Antarctic marine ecosystem: practical implementation of the Convention on the Conservation of the Antarctic Marine Living Resources (CCAMLR). *ICES Journal of Marine Science* 57: 778–791.

Everson I (ed.) (2000) *Krill: Biology, Ecology and Fisheries*. Oxford: Blackwell Science.

Everson I (2000) Introducing krill. In: Everson I (ed.) *Krill: Biology, Ecology and Fisheries*. Oxford: Blackwell Science.

Falk-Petersen S, Hagen W, Kattner G, Clarke A and Sargent J (2000) Lipids, trophic relationship, and biodiversity in Arctic and Antarctic krill. *Canadian Journal of Fisheries and Aquatic Sciences* 57: 178–191.

Mauchline JR (1980) The biology of the Euphausids. *Advances in Marine Biology* 18: 371–677.

Mauchline JR and Fisher LR (1969) The biology of the Euphausids. *Advances in Marine Biology* 7: 1–454.

Miller D and Hampton I (1989) *Biology and Ecology of the Antarctic Krill*. BIOMASS Scientific Series, 9. Cambridge: SCAR & SCOR.

Murphy EJ, Watkins JL, Reid K *et al.* (1998) Interannual variability of the South Georgia marine ecosystem: physical and biological sources of variation. *Fisheries Oceanography* 7: 381–390.

Siegel V and Nichol S (2000) Population parameters. In: Everson I (ed.) *Krill: Biology, Ecology and Fisheries*. Oxford: Blackwell Science.

KUROSHIO AND OYASHIO CURRENTS

B. Qiu, University of Hawaii at Manoa, Hawaii, USA

Introduction

The Kuroshio and Oyashio Currents are the western boundary currents in the wind-driven, subtropical and subarctic circulations of the North Pacific Ocean. Translated from Japanese, Kuroshio literally means black ('kuro') stream ('shio') owing to the blackish – ultramarine to cobalt blue – color of its water. The 'blackness' of the Kuroshio Current stems from the fact that the downwelling-dominant subtropical North Pacific Ocean is low in biological productivity and is devoid of detritus and other organic material in the surface water. The subarctic North Pacific Ocean, on the other hand, is dominated by upwelling. The upwelled, nutrient-rich water feeds the Oyashio from the north and leads to its nomenclature, parent ('oya') stream ('shio').

The existence of a western boundary current to compensate for the interior Sverdrup flow is well understood from modern wind-driven ocean circulation theories. Individual western boundary currents, however, can differ greatly in their mean flow and variability characteristics due to different bottom topography, coastline geometry, and surface wind patterns that are involved. For example, the bimodal oscillation of the Kuroshio path south of Japan is a unique phenomenon detected in no other western boundary current of the world oceans. Similarly, interaction with the semi-enclosed and often ice-covered marginal seas and excessive precipitation over evaporation in the subarctic North Pacific Ocean make the Oyashio Current considerably

different from its counterpart in the subarctic North Atlantic Ocean, the Labrador Current.

Because the Kuroshio and Oyashio Currents exert a great influence on the fisheries, hydrography, and meteorology of countries surrounding the western North Pacific Ocean, they have been the focus of a great amount of observation and research in the past. This article will provide a brief review of the dynamic aspects of the observed Kuroshio and Oyashio Currents: their origins, their mean flow patterns, and their variability on seasonal-to-interannual timescales. The article consists of two sections, the first focusing on the Kuroshio Current and the second on the Oyashio Current. Due to the vast geographical areas passed by the Kuroshio Current (**Figure 1**), the first section is divided into three subsections: the region upstream of the Tokara Strait, the region south of Japan, and the Kuroshio Extension region east of the Izu Ridge. As will become clear, the Kuroshio Current exhibits distinct characteristics in each of these geographical locations owing to the differing governing physics.

The Kuroshio Current

Region Upstream of the Tokara Strait

The Kuroshio Current originates east of the Philippine coast where the westward flowing North Equatorial Current (NEC) bifurcates into the northward-flowing Kuroshio Current and the southward-flowing Mindanao Current. At the sea surface, the NEC bifurcates nominally at 12°N–13°N, although this bifurcation latitude can change interannually from 11°N to 14.5°N. The NEC's bifurcation tends to migrate to the north during El Niño years and to the south during La Niña years. Below the sea surface, the NEC's bifurcation tends to shift northward with increasing depth. This tendency is due to the fact that the southern limb of the wind-driven subtropical gyre in the North Pacific shifts to the north with increasing depth.

Branching northward from the NEC, the Kuroshio Current east of the Philippine coast has a mean geostrophic volume transport, referenced to 1250 dbar, of 25 Sv (1 Sverdrup = $10^6 \, \mathrm{m}^3 \, \mathrm{s}^{-1}$). Seasonally, the Kuroshio transport at this upstream
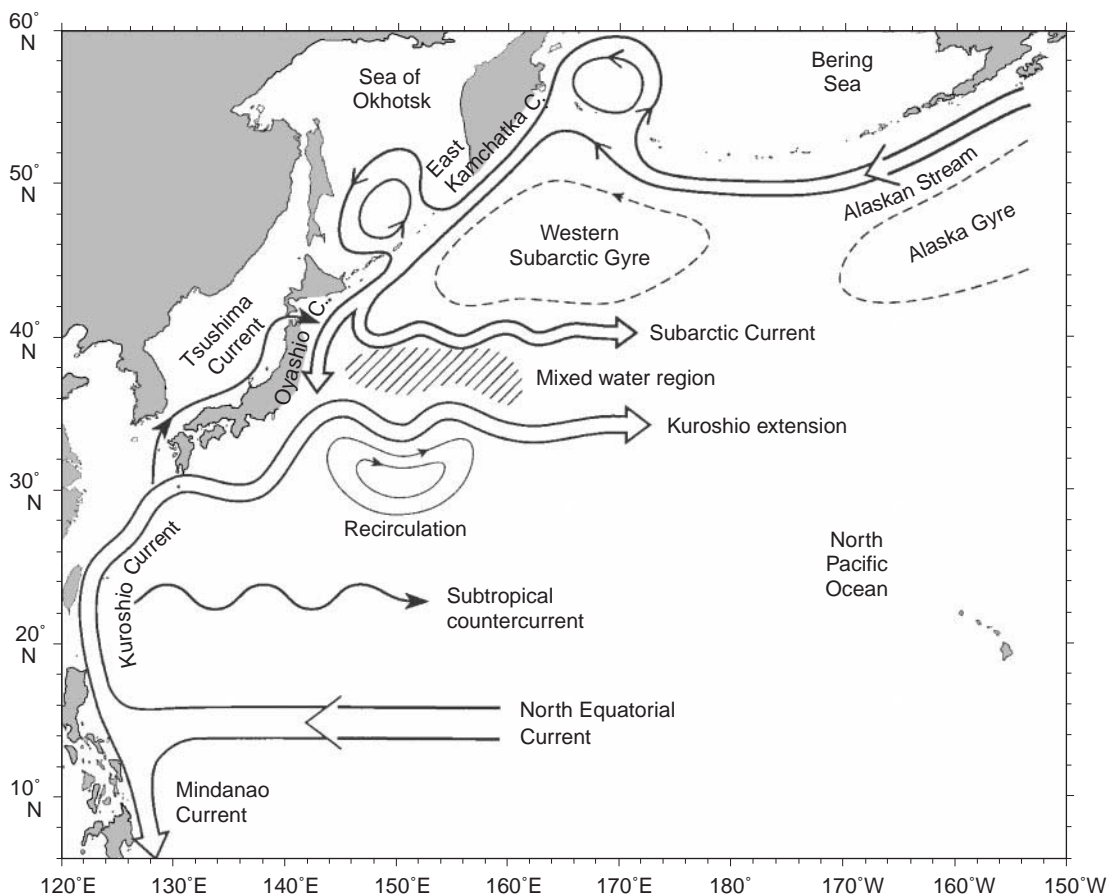

Figure 1   Schematic current patterns associated with the subtropical and subarctic gyres in the western North Pacific Ocean.

location has a maximum (∼ 30 Sv) in spring and a minimum (∼ 19 Sv) in fall. Similar seasonal cycles are also found in the Kuroshio's transports in the East China Sea and across the Tokara Strait.

As the Kuroshio Current flows northward passing the Philippine coast, it encounters the Luzon Strait that connects the South China Sea with the open Pacific Ocean (**Figure 2**). The Luzon Strait has a width of 350 km and is 2500 m deep at its deepest point. In winter, part of the Kuroshio water has been observed to intrude into the Luzon Strait and form a loop current in the northern South China Sea (see the dashed line in **Figure 2**). The loop current can reach as far west as 117°E, where it is blocked by the presence of the shallow shelf break off the south-east coast of China. The formation of the loop current is probably due to the north-east monsoon, prevailing from November to March, which deflects the surface Kuroshio water into the northern South China Sea. During the summer months from May to September when the south-west monsoon prevails, the Kuroshio Current passes the Luzon Strait without intrusion.

In the latitudinal band east of Taiwan (22°N–25°N), the northward-flowing Kuroshio Current has been observed to be highly variable in recent years. Repeat hydrographic and moored current meter measurements between Taiwan and the southernmost Ryukyu island of Iriomote show that the variability of the Kuroshio path and transport here are dominated by fluctuations with a period of 100 days. These observed fluctuations are caused by impinging energetic cyclonic and anticyclonic eddies migrating from the east. The Subtropical Countercurrent (STCC) is found in the latitudinal band of 22°N–25°N in the western North Pacific. The STCC, a shallow eastward-flowing current, is highly unstable due to its velocity shear with the underlying, westward-flowing NEC. The unstable waves generated by the instability of the STCC-NEC system tend to move westward while growing in amplitude. The cyclonic and anticyclonic eddies that impinge upon the Kuroshio east of Taiwan are
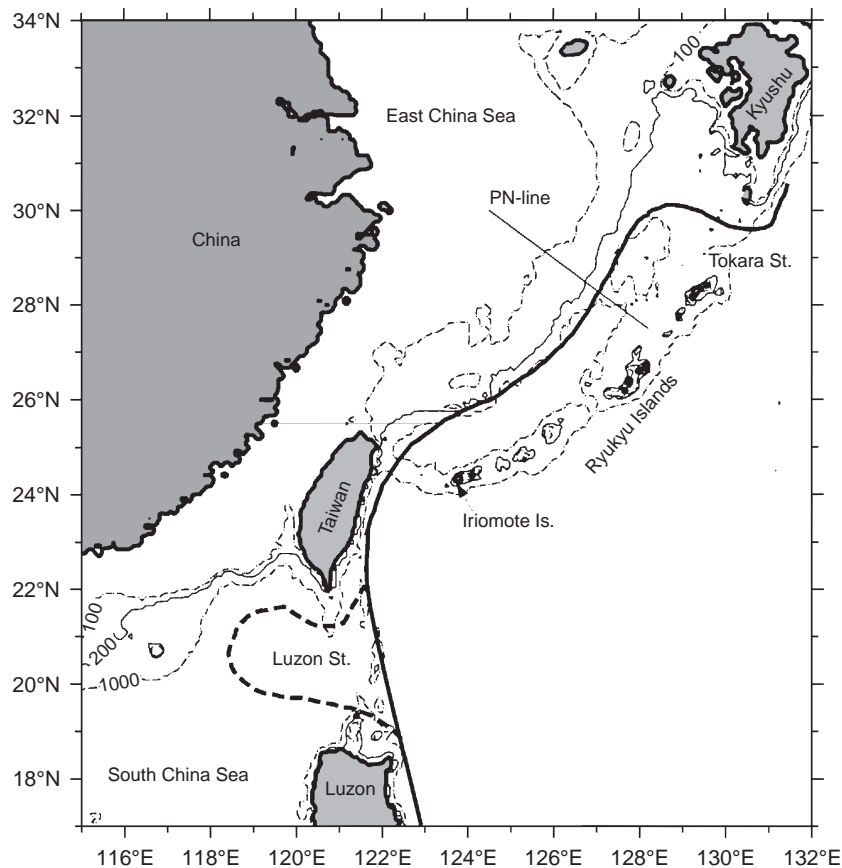

Figure 2 Schematic representation of the mean Kuroshio path (solid thick line) along the North Pacific western boundary. The thick dashed line south of Taiwan denotes the wintertime branching of the Kuroshio water into the Luzon Strait in the form of a loop current. PN-line denotes the repeat hydrographic section across which long-term Kuroshio volume transport is monitored (see **Figure 4**). Selective isobaths of 100 m, 200 m, and 1000 m are depicted.
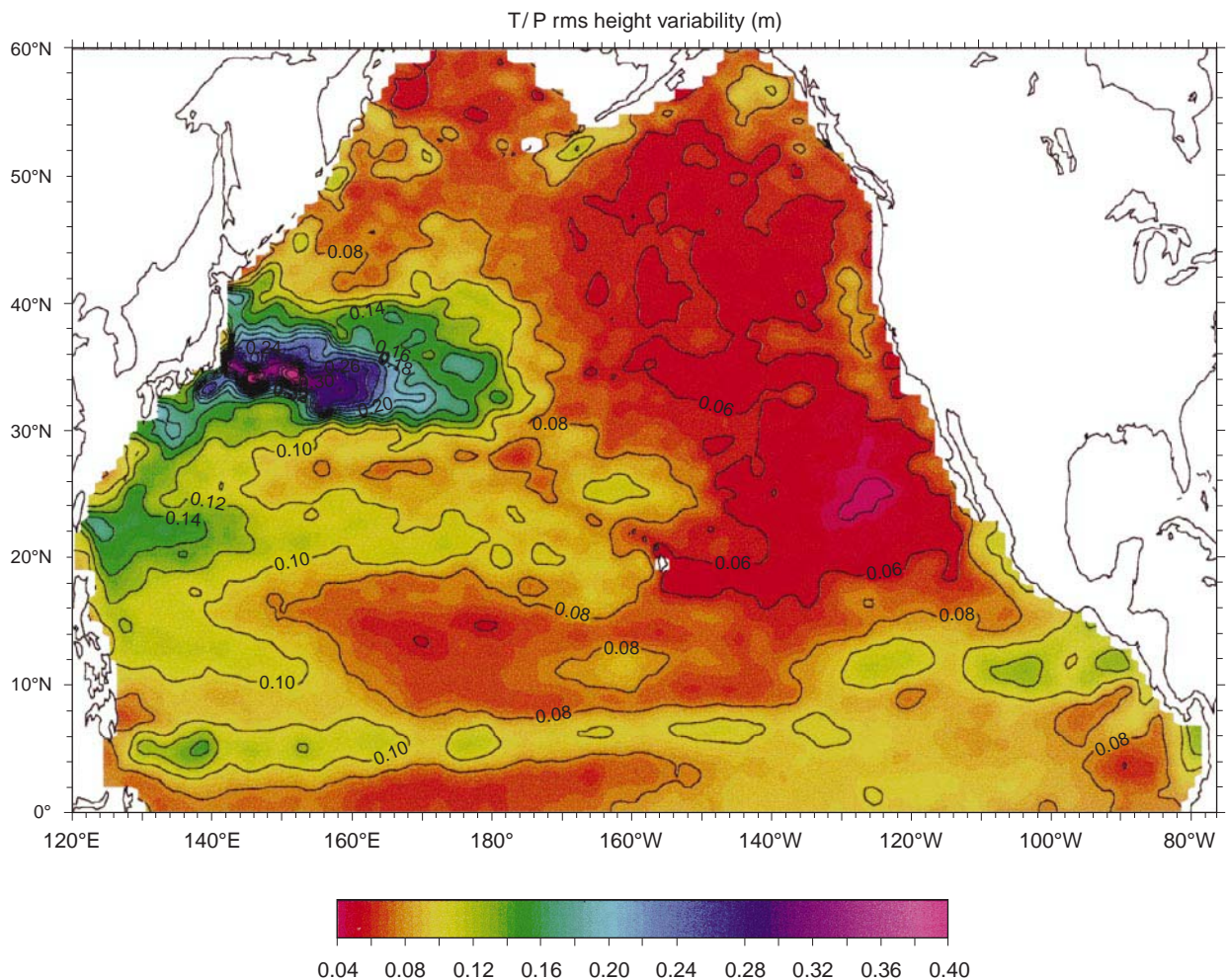
Figure 3 Map of the root-mean-square (rms) sea surface height variability in the North Pacific Ocean, based on the TOPEX/POSEIDON satellite altimetric measurements from October 1992 to December 1997. Maximum rms values of > 0.4 m are found in the upstream Kuroshio Extension region south east of Japan. Sea surface height variability is also high in the latitudinal band east of Taiwan. (Adapted with permission from Qiu B (1999) Seasonal eddy field modulation of the North Pacific Subtropical Countercurrent: TOPEX/Poseidon observations and theory. *Journal of Physical Oceanography* 29: 2471–2486.)

results of these large-amplitude unstable waves. Indeed, satellite measurements of the sea level (**Figure 3**) show that the Kuroshio east of Taiwan has higher eddy variability than either its upstream counterpart along the Philippine coast or its downstream continuation in the East China Sea.

The Kuroshio Current enters the East China Sea through the passage between Taiwan and Iriomote Island. In the East China Sea, the Kuroshio path follows closely along the steep continental slope. Across the PN-line in the East China Sea (see **Figure 2** for its location), repeat hydrographic surveys have been conducted on a quarterly basis by the Japan Meteorological Agency since the mid-1950s. Based on the measurements from 1955 to 1998, the volume transport of the Kuroshio across this section has a mean of 24.6 Sv and a seasonal cycle with 24.7 Sv in winter, 25.4 Sv in spring, 25.2 Sv in summer, and 22.8 Sv in fall, respectively. In addition to this seasonal signal, large transport changes on longer timescales are also detected across this section (see **Figure 4**). One signal that stands out in the time-series of **Figure 4** is the one with the decadal timescale. Specifically, the Kuroshio transport prior to 1975 was low on average (22.5 Sv), whereas the mean transport value increased to 27.0 Sv after 1975. This decadal signal in the Kuroshio's volume transport is associated with the decadal Sverdrup transport change in the subtropical North Pacific Ocean.

Although the main body of the Kuroshio Current in the East China Sea is relatively stable due to the topographic constraint, large-amplitude meanders are frequently observed along the density front of
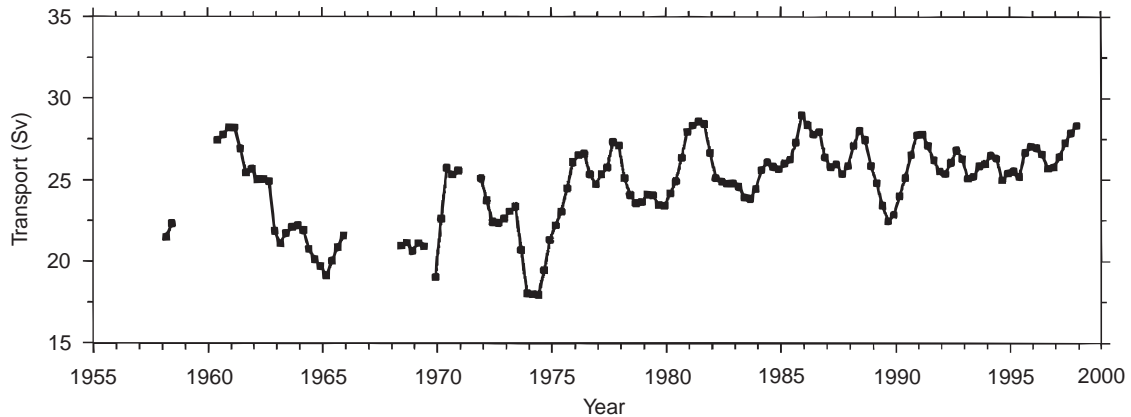
Figure 4 Time-series of the geostrophic volume transport of the Kuroshio across the PN-line in the East China Sea (see **Figure 2** for its location). Reference level is at 700 dbar. Quarterly available transport values have been low-pass filtered by the 1-year running mean averaging. (Data courtesy of Dr M. Kawabe of the University of Tokyo.)

the Kuroshio Current. The density front marks the shoreward edge of the Kuroshio Current and is located nominally along the 200 m isobath in the East China Sea. The frontal meanders commonly originate along the upstream Kuroshio front north east of Taiwan and they evolve rapidly while propagating downstreamward. The frontal meanders have typical wavelengths of 200–350 km, wave periods of 10–20 days, and downstreamward phase speeds of $10–25 \, cm \, s^{-1}$. When reaching the Tokara Strait, the fully developed frontal meanders can shift the path of the Kuroshio Current in the strait by as much as 100 km.

Around 128°E–129°E and 30°N, the Kuroshio Current detaches from the continental slope and veers to the east toward the Tokara Strait. Notice that this area is also where part of the Kuroshio water is observed to intermittently penetrate northward onto the continental shelf to feed the Tsushima Current. The frontal meanders of the Kuroshio described above are important for the mixing and water mass exchanges between the cold, fresh continental shelf water and the warm, saline Kuroshio water along the shelf break of the East China Sea. It is this mixture of the water that forms the origin of the Tsushima Current. The volume transport of the Tsushima Current is estimated at 2 Sv.

Region South of Japan

The Kuroshio Current enters the deep Shikoku Basin through the Tokara Strait. Combined surface current and hydrographic observations show that the Kuroshio's volume transport through the Tokara Strait is about 30 Sv. Inference of transport from the sea level measurements suggests that the Kuroshio's

transport across the Tokara Strait is maximum in spring/summer and minimum in fall, a seasonal cycle similar to that found in the upstream Kuroshio Current. Further downstream, offshore of Shikoku, the volume transport of the Kuroshio has a mean value of 55 Sv. This transport increase of the Kuroshio in the deep Shikoku Basin is in part due to the presence of an anticyclonic recirculation gyre south of the Kuroshio. Subtracting the contribution from this recirculation reduces the mean eastward transport to 42 Sv. Notice that this 'net' eastward transport of the Kuroshio is still larger than its inflow transport through the Tokara Strait. This increased transport, ∼ 12 Sv, is probably supplied by the north-eastward-flowing current that has been occasionally observed along the eastern flank of the Ryukyu Islands. Near 139°E, the Kuroshio Current encounters the Izu Ridge. Due to the shallow northern section of the ridge, the Kuroshio Current exiting the Shikoku Basin is restricted to passing the Izu Ridge at either around 34°N where there is a deep passage, or south of 33°N where the ridge height drops.

On interannual timescales, the Kuroshio Current south of Japan is known for its bimodal path fluctuations. The 'straight path', shown schematically by path A in **Figure 5**, denotes when the Kuroshio flows closely along the Japan coast. The 'large-meander path', shown by path B in **Figure 5**, signifies when the Kuroshio takes a detouring offshore path. In addition to these two stable paths, the Kuroshio may take a third, relatively stable path that loops southward over the Izu Ridge. This path, depicted as path C in **Figure 5**, is commonly observed during transitions from a meandering state to a straight-path state. As the meander path of the Kuroshio can migrate spatially, a useful way of
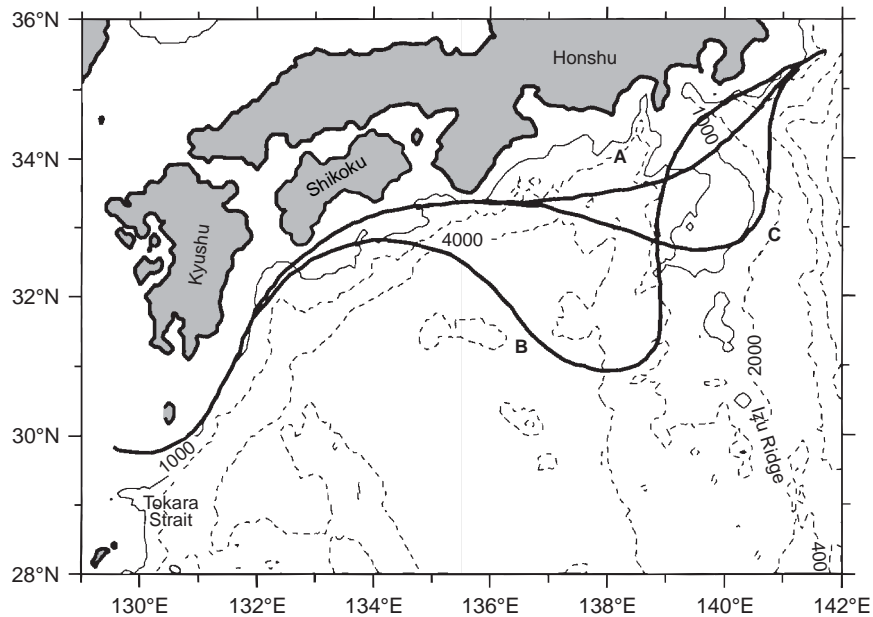
Figure 5 Schematic stable paths of the Kuroshio Current south of Japan. (Adapted with permission from Kawabe M (1985) Sea level variations at the Izu Islands and typical stable paths of the Kuroshio. *Journal of the Oceanography Society of Japan* 41: 307–326.) Selective isobaths of 1000 m, 2000 m, 4000 m, 6000 m, and 8000 m are included.

indexing the Kuroshio path is to use the mean distance of the Kuroshio axis from the Japan coast from 132°E to 140°E. South of Japan, the Kuroshio axis is well represented by the 16°C isotherm. Based on this representation and seasonal water temperature measurements, **Figure 6** shows the time-series of the Kuroshio path index from 1955 to 1998. A low index in **Figure 6** denotes a straight path, and a high index denotes an offshore meandering path of the Kuroshio. From 1955 to 1998, the Kuroshio large meanders occurred in 1959–62, 1975–79,

1982–88, and 1990. Clearly, the large-meanders occurrence is aperiodic. Once formed, the meander state can persist over a period ranging from a year to a decade. In contrast, transitions between the meander and straight-path states are rapid, often completed over a period of several months. It is worth noting that development of the large meanders is often preceded by the appearance of a small meander south of Kyushu, which migrates eastward and becomes stationary after reaching 136°E.
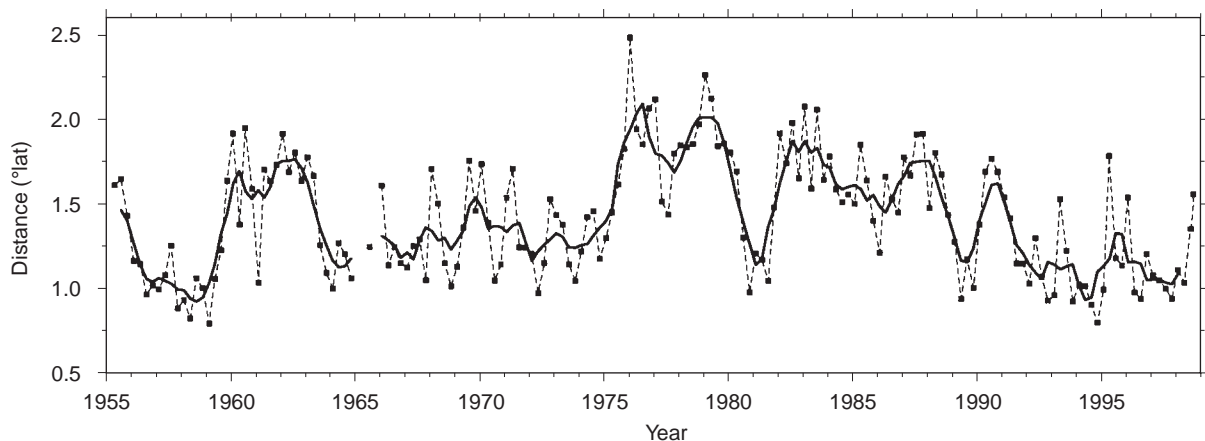

Figure 6 Time-series of the Kuroshio path index from 1955 to 1998, where the Kuroshio path index is defined as the offshore distance of the Kuroshio axis (inferred from the 16°C isotherm at the 200 m depth) averaged from 132° to 140°E. Solid dots denote the seasonal index values and the solid line indicates the annual average. (Adapted with permission from Qiu B and Miao W (2000) Kuroshio path variations south of Japan: Bimodality as a self-sustained internal oscillation. *Journal of Physical Oceanography* 30: 2124–2137.)

Several mechanisms have been proposed to explain the bimodal path variability of the Kuroshio south of Japan. Most studies have examined the relationship between the Kuroshio's path pattern and the changes in magnitude of the Kuroshio's upstream transport. Earlier studies of the Kuroshio path bimodality interpreted the meandering path as stationary Rossby lee wave generated by the protruding coastline of Kyushu. With this interpretation, the Kuroshio takes a meander path when the upstream transport is small and a straight path when it is large. By taking into account the realistic inclination of the Japan coast from due east, more recent studies have provided the following explanation. When the upstream transport is small, the straight path is stable as a result of the planetary vorticity acquired by the north-eastward-flowing Kuroshio being balanced by the eddy dissipation along the coast. When the upstream transport is large, positive vorticity is excessively generated along the Japan coast, inducing the meander path to develop downstream. In the intermediate transport range, the Kuroshio is in a multiple equilibrium state in which the meandering and straight paths coexist. Transitions between the two paths in this case are determined by changes in the upstream transport (e.g. the transition from a straight path to a meander path requires an increase in upstream transport).

A comparison between the Kuroshio path variation (**Figure 6**) and the Kuroshio's transport in the upstream East China Sea (**Figure 4**) shows that the 1959–62 large-meander event does correspond to a large upstream transport. However, this correspondence becomes less obvious after 1975, as there were times when the upstream transport was large, but no large meander was present. Assuming that the upstream Kuroshio transport after 1975 is in the multiple equilibrium regime, the correspondence between the path transition and the temporal change in the upstream transport (e.g. the required transport increase for the transition from a straight path to a meander path) is also inconclusive from the time-series presented in **Figures 4** and **6**. Given the low frequency and irregular nature of the Kuroshio path changes, future studies based on longer transport measurements are needed to further clarify the physics underlying the Kuroshio path bimodality.

Downstream Extension Region

After separating from the Japan coast at 140°E and 35°N, the Kuroshio enters the open basin of the North Pacific Ocean where it is renamed the Kuroshio Extension. Free from the constraint of coastal boundaries, the Kuroshio Extension has been observed to be an eastward-flowing inertial jet accompanied by large-amplitude meanders and energetic pinched-off eddies. **Figure 7** shows the mean temperature map at 300 m depth, in which the axis of the Kuroshio Extension is well represented by the 12°C isotherm. An interesting feature of the Kuroshio Extension east of Japan is the existence of two quasi-stationary meanders with their ridges located at 144°E and 150°E, respectively. The presence of these meanders along the mean path of the Kuroshio Extension has been interpreted as standing Rossby lee waves generated by the presence of the Izu Ridge. A competing theory also exists that regards the quasi-stationary meanders as being steered by the eddy-driven abyssal mean flows resulting from instability of the Kuroshio Extension jet.
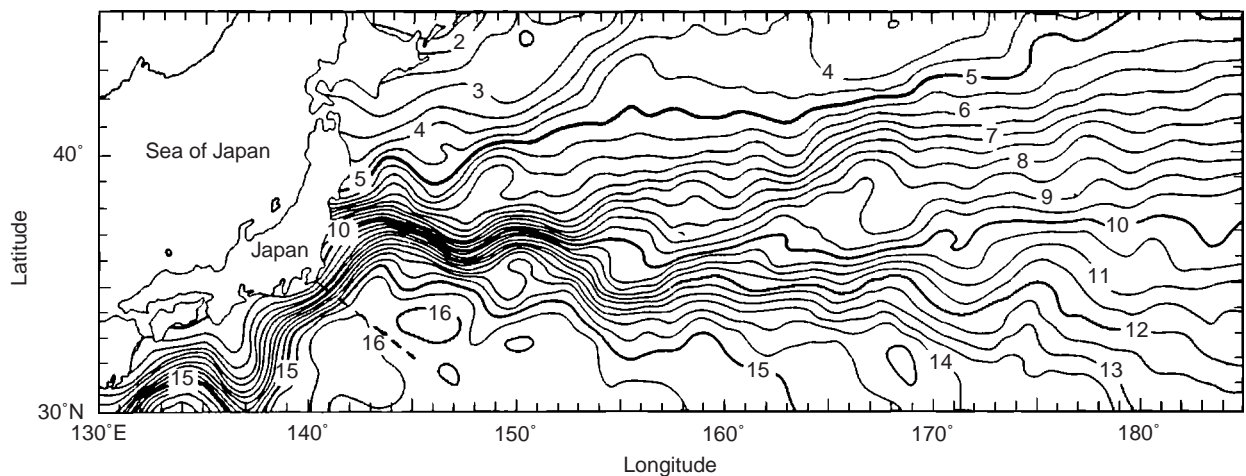

Figure 7 Mean temperature map (°C) at the 300 m depth from 1976 to 1980. (Adapted with permission from Mizuno K and White WB (1983) Annual and interannual variability in the Kuroshio Current System. *Journal of Physical Oceanography* 13: 1847–1867.)

Near 159°E, the Kuroshio Extension encounters the Shatsky Rise where it often bifurcates. The main body of the Kuroshio Extension continues eastward, and a secondary branch tends to extend north-eastward to 40°N, where it joins the eastward-moving Subarctic Current. After overriding the Emperor Seamounts along 170°E, the mean path of the Kuroshio Extension becomes broadened and instantaneous flow patterns often show a multiple-jet structure associated with the eastward-flowing Kuroshio Extension. East of the dateline, the distinction between the Kuroshio Extension and the Subarctic Current is no longer clear, and together they form the broad, eastward-moving North Pacific Current.

As demonstrated in **Figure 3**, the Kuroshio Extension region has the highest level of eddy variability in the North Pacific Ocean. From the viewpoint of wind-driven ocean circulation, this high eddy variability is to be expected. Being a return flow compensating for the wind-driven subtropical interior

circulation, the Kuroshio originates at a southern latitude where the ambient potential vorticity (PV) is relatively low. For the Kuroshio to smoothly rejoin the Sverdrup interior flow at the higher latitude, the low PV acquired by the Kuroshio in the south has to be removed by either dissipative or nonlinear forces along its western boundary path. For the narrow and swift Kuroshio Current, the dissipative force is insufficient to remove the low PV anomalies. The consequence of the Kuroshio's inability to effectively diffuse the PV anomalies along its path results in the accumulation of low PV water in its extension region, which generates an anticyclonic recirculation gyre and provides an energy source for flow instability. Due to the presence of the recirculation gyre (**Figure 8**), the eastward volume transport of the Kuroshio Extension can reach as high as 130 Sv south east of Japan. This is more than twice the maximum Sverdrup transport of about 50 Sv in the subtropical North Pacific. The inflated eastward transport is due to the presence of the recirculating
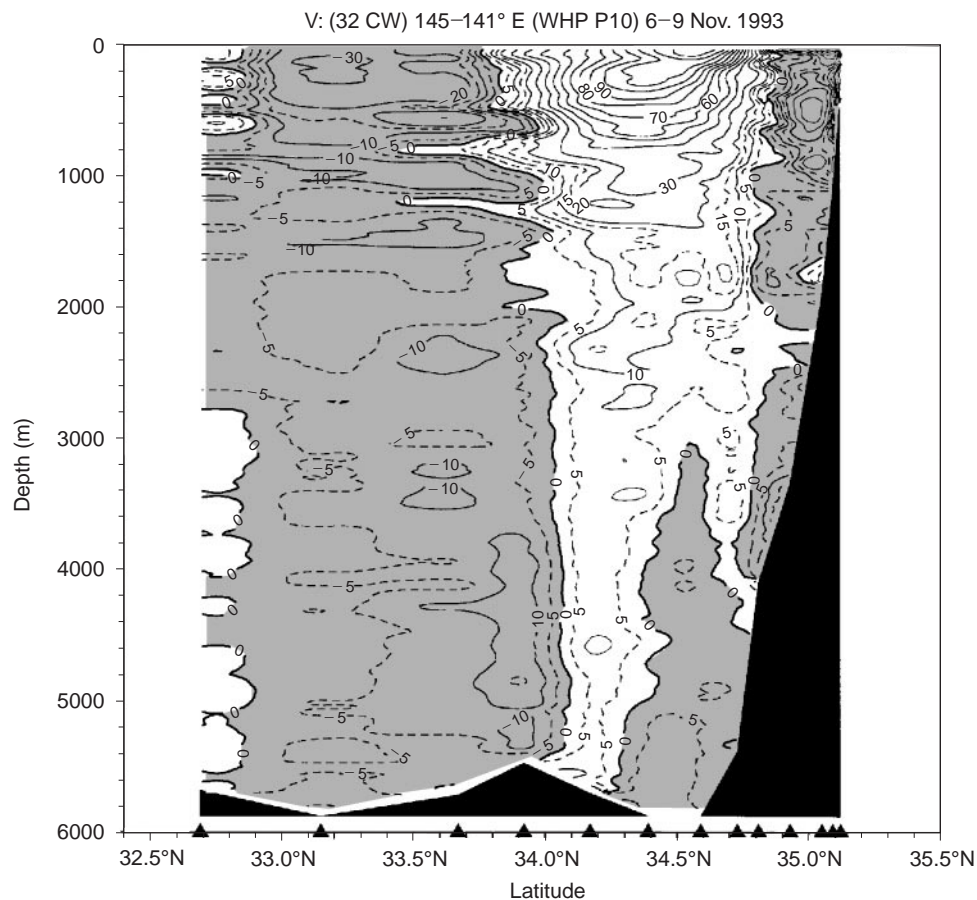

Figure 8 North-eastward velocity profile from lowered acoustic Doppler current meter profiler (ADCP) measurements along the WOCE P10 line south east of Japan in November 1993 (see the dashed line in **Figure 7** for its location). Units are cm s^{-1} and south-westward flow is shaded. (Figure courtesy of Drs E. Firing and P. Hacker of the University of Hawaii.)

flow to the south of the Kuroshio Extension. Although weak in surface velocity, **Figure 8** shows that the recirculating flow has a strong barotropic (i.e. depth-independent) component. As a consequence, the volume transport of the recirculation gyre in this case is as large as 80 Sv.

In addition to the high meso-scale eddy variability, the Kuroshio Extension also exhibits large-scale changes on interannual timescales. **Figure 9A** and **B** compares the sea surface height field in the Kuroshio Extension region in November 1992 with that in November 1995. In 1992, the Kuroshio Extension had a coherent zonal-jet structure extending beyond the dateline. The zonal mean axis

position of the Kuroshio Extension from 141°E to 180°E in this case was located north of 35°N. In contrast, the jet-like structure in 1995 was no longer obvious near 160°E and the zonal mean axis position shifted to 34°N. Note that the changes in the zonal mean axis position of the Kuroshio Extension have interannual timescales (**Figure 9C**) and are associated with the changes in the strength of the southern recirculation gyre. As the recirculation gyre intensifies (as in 1992), it elongates zonally, increasing the zonal mean eastward transport of the Kuroshio Extension and shifting its mean position northward. When the recirculation gyre weakens (as in 1995), it decreases the eastward transport of the
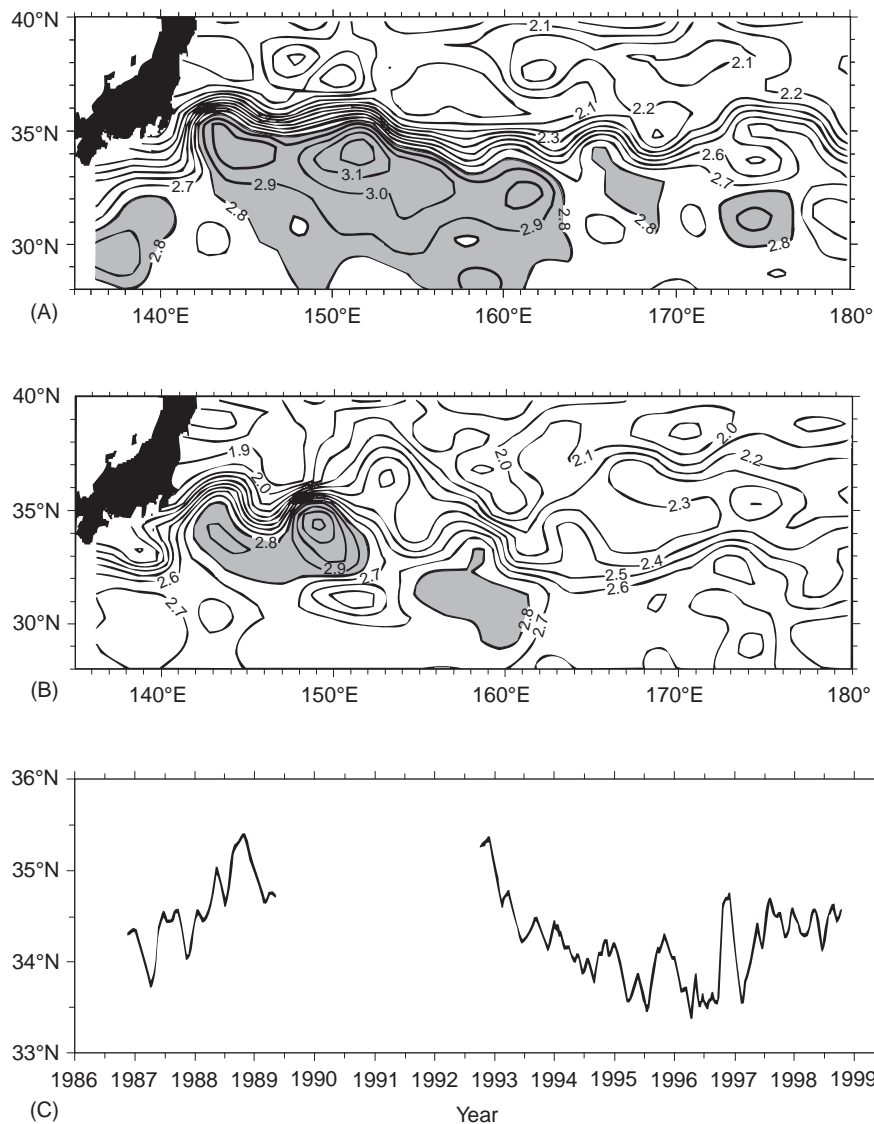

Figure 9   Sea surface height maps on (A) 20 November 1992 and (B) 15 November 1995 from the TOPEX/POSEIDON altimeter measurements. (C) Time-series of the mean axis position of the Kuroshio Extension from 141°E to 180°. (Adapted with permission from Qiu B (2000) Interannual variability of the Kuroshio Extension system and its impact on the wintertime SST field. *Journal of Physical Oceanography* 30: 1486–1502.)

Kuroshio Extension and shifts its zonal mean position southward. At present, the cause of the low-frequency changes of the recirculation gyre is unclear.

The Oyashio Current

Due to the southward protrusion of the Aleutian Islands, the wind-driven subarctic circulation in the North Pacific Ocean can be largely divided into two cyclonic subgyres: the Alaska Gyre to the east of the dateline and the Western Subarctic Gyre to the west (**Figure 1**). To the north, these two subgyres are connected by the Alaskan Stream, which flows south-westward along the Aleutian Islands as the western boundary current of the Alaska Gyre. Near the dateline, the baroclinic volume transport of the Alaskan Stream in the upper 3000 m layer is estimated at about 15–20 Sv. As the Alaskan Stream flows further westward, the deep passages between 168°E and 172°E along the western Aleutian Islands allow part of the Alaskan Stream to enter the Bering Sea. In the deep part of the Bering Sea, the intruding Alaskan Stream circulates anticlockwise and forms the Bering Sea Gyre. The western limb of the Bering Sea Gyre becomes the East Kamchatka Current, which flows south-westward along the east coast of the Kamchatka Peninsula. The remaining part of the Alaskan Stream continues westward along the southern side of the Aleutian Islands and upon reaching the Kamchatka Peninsula, it joins the East Kamchatka Current as the latter exits the Bering Sea.

As the East Kamchatka Current continues south-westward and passes along the northern Kuril Islands, some of its water permeates into the Sea of Okhotsk. Inside the deep Kuril Basin in the Sea of Okhotsk, the intruding East Kamchatka Current water circulates in a cyclonic gyre. Much of this intruding water moves out of the Sea of Okhotsk through the Bussol Strait (46.5°N, 151.5°E), where it joins the rest of the south-westward-flowing East Kamchatka Current. The East Kamchatka Current is renamed the Oyashio Current south of the Bussol Strait. Because of the intrusion in the Sea of Okhotsk, the water properties of the Oyashio Current are different from those in the upstream East Kamchatka Current. For example, the mesothermal water present in the East Kamchatka Current (i.e. the subsurface maximum temperature water appearing in the halocline at a depth of 150–200 m) is no longer observable in the Oyashio. While high dissolved oxygen content is confined to above the halocline in the upstream East Kamchatka Current, elevated dissolved oxygen values can be found throughout the upper 700 m depth of the Oyashio water.

The baroclinic volume transport of the Oyashio Current along the southern Kuril Islands and off Hokkaido has been estimated at 5–10 Sv from the geostrophic calculation with a reference level of no-motion at 1000 or 1500 m. Combining moored current meter and CTD (conductivity-temperature-depth) measurements, more recent observations along the continental slope south east of Hokkaido show that the Oyashio Current has a well-defined annual cycle: the flow tends to be strong, reaching from surface to bottom, in winter/spring, and it is weaker and confined to the layer shallower than 2000 m in summer and fall. The total (baroclinic + barotropic) volume transport reaches 20–30 Sv in winter and spring, whereas it is only 3–4 Sv in summer and fall. This annual signal in the Oyashio's total transport is in agreement with the annual signal in the Sverdrup transport of the wind-driven North Pacific subArctic gyre.

After flowing south-westward along the coast of Hokkaido, the Oyashio Current splits into two paths. One path veers offshoreward and contributes to the east-north-eastward-flowing SubArctic Current. This path can be recognized in **Figure 10** by the eastward-veering isotherms along 42°N south east of Hokkaido. Because the Oyashio Current brings water of subarctic origin southward, the Subarctic Current is accompanied by a distinct temperature-salinity front between cold, fresher water to the north and warm, saltier water of subtropical origin to the south. This water mass front, referred to as the Oyashio Front or the Subarctic Front, has indicative temperature and salinity values of 5°C and 33.8 PSU at the 100 m depth. Across 165°E, combined moored current meter and CTD measurements show that the Subarctic Current around 41°N has a volume transport of 22 Sv in the upper 1000 m layer.

The second path of the Oyashio Current continues southward along the east coast of Honshu and is commonly known as the first Oyashio intrusion. As shown in **Figure 10**, an addition to this primary intrusion along the coast of Honshu, the southerly Oyashio intrusion is also frequently observed further offshore along 147°E. This offshore branch is commonly known as the second Oyashio intrusion. The annual mean first Oyashio intrusion east of Honshu reaches on average the latitude 38.7°N, although in some years it can penetrate as far south as 37°N (see **Figure 11**). In addition to the year-to-year fluctuations, **Figure 11** shows that there is a trend for the Oyashio Current to penetrate farther southward after the mid-1970s. Both this
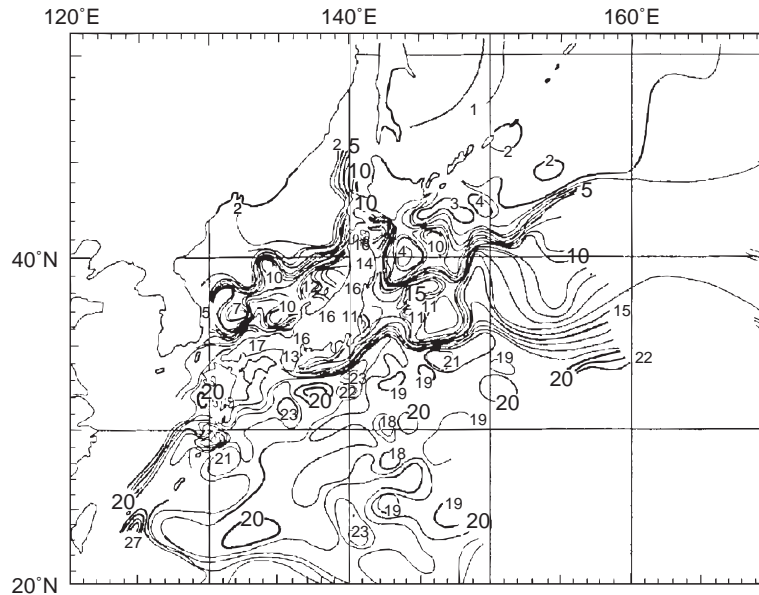
Figure 10 Water temperature map at the 100 m depth in September 1989 compiled by the Japan Meteorological Agency. Contour interval is 1°C.

long-term trend and the interannual changes in the Oyashio's intrusions seem to be related to the changes in the intensity of the Aleutian low atmospheric pressure system and the southward shift in the position of the mid-latitude westerlies. It is worth noting that the anomalous southward intrusion of the Oyashio Current not only influences the hydrographic conditions east of Honshu, it also affects the environmental conditions in the fishing ground and the regional climate (e.g. an anomalous southward intrusion tends to decrease the air temperature over eastern Japan).

Concluding Remarks

Because the Kuroshio and Oyashio Currents transport large amounts of water and heat efficiently in the meridional direction, there has been heightened interest in recent years in understanding the dynamic roles played by the time-varying Kuroshio and Oyashio Currents in influencing the climate through sea surface temperature (SST) anomalies. Indeed, outside the eastern equatorial Pacific Ocean, the largest SST variability on the interannual-to-decadal timescale in the North Pacific Ocean resides in the
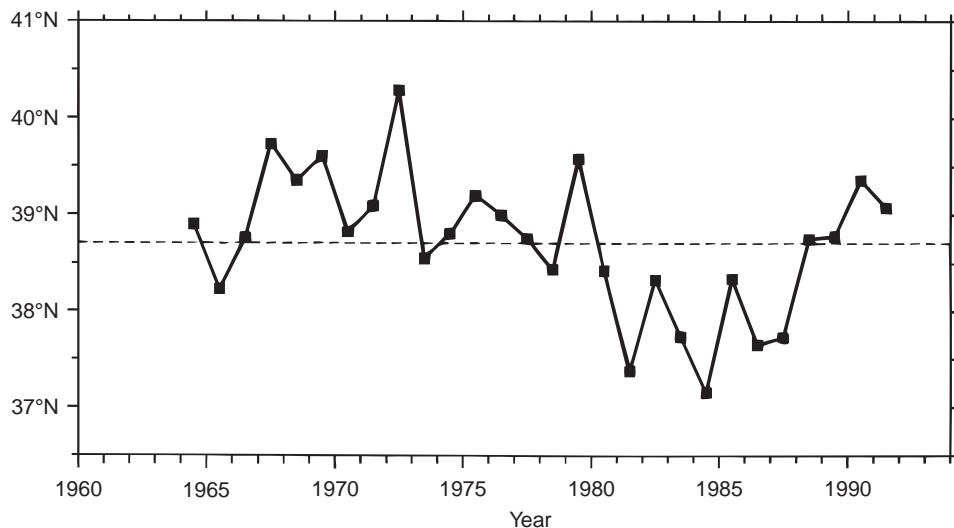

Figure 11 Time-series of the annually averaged southernmost latitude of the first Oyashio intrusion east of Honshu. The dashed line shows the mean latitude (38.7°N) over the period from 1964 to 1991. (Data courtesy of Dr K. Hanawa of Tohoku University.)

Kuroshio Extension and the Oyashio outflow regions (**Figure 12**). Large-scale changes in the Kuroshio and Oyashio current systems can affect the SST anomaly field through warm/cold water advection, upwelling through the base of the mixed layer, and changes in the current paths and the level of the meso-scale eddy variability. At present, the relative roles played by these various physical processes are not clear.

This article summarizes many observed aspects of the Kuroshio and Oyashio Current systems, although due to the constraints of space, important subjects such as the water mass transformation processes in regions surrounding the Kuroshio and Oyashio and the impact of the Kuroshio and Oyashio variability upon the oceanographic conditions in coastal and marginal sea areas have not been addressed. It is worth emphasizing that our knowledge of the Kuroshio and Oyashio Currents has increased significantly due to the recent World Ocean Circulation Experiment (WOCE) program (observational phase: 1990–1997). Fortunately, many of the observational programs initiated under the WOCE program are being continued. With results from these new observations, we can expect an improved description of the Kuroshio and Oyashio Current systems in the near future, especially of the variability with timescales longer than those described in this article.
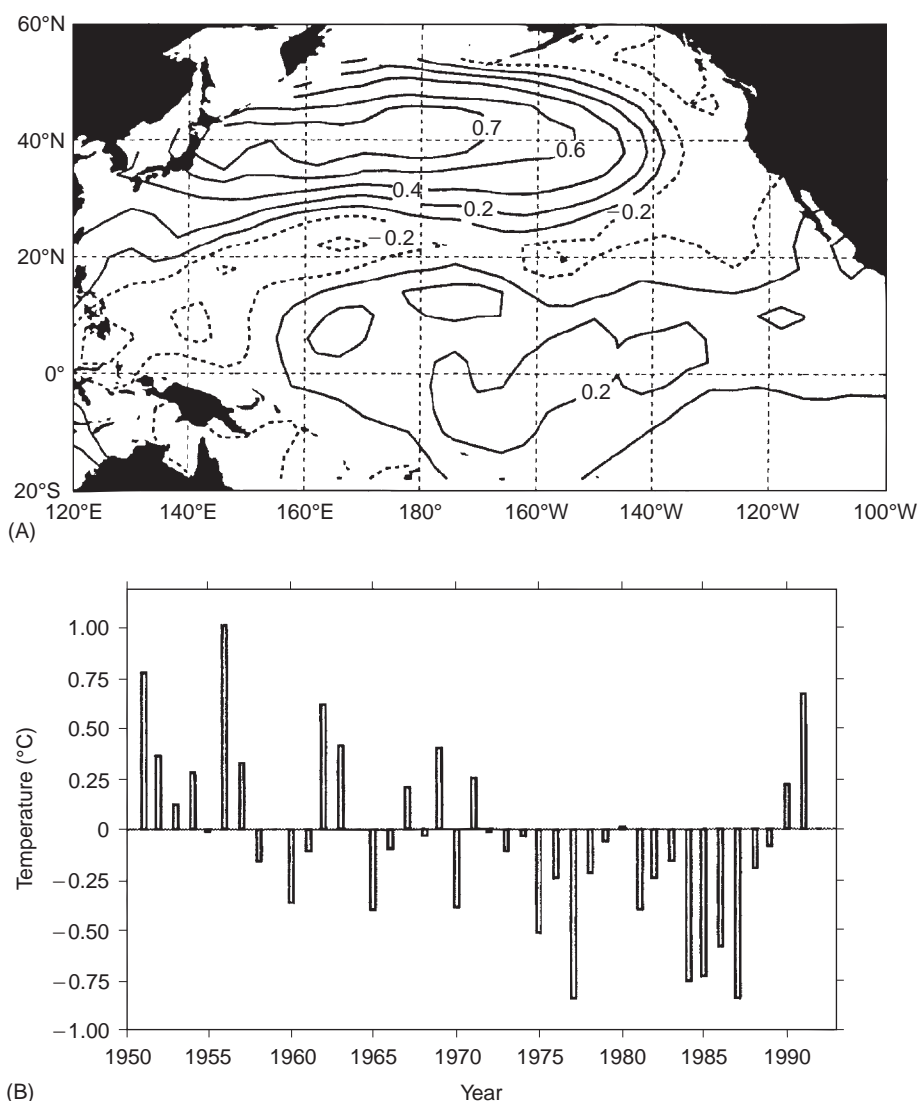
Figure 12 (A) Spatial pattern of the second empirical orthogonal function (EOF) mode of the wintertime sea surface temperature anomalies (1950–1992) in the Pacific Ocean. This mode explains 11% of the variance over the domain. (B) Time-series of the wintertime sea surface temperature anomalies averaged in the Kuroshio-Oyashio outflow region (32°N–46°N, 136°E–176°W). (Adapted with permission from Deser C and Blackmon ML (1995) On the relationship between tropical and North Pacific sea surface variations. *Journal of Climate* 8: 1677–1680.)

See also

Abyssal Currents. Okhotsk Sea Circulation. Pacific Ocean Equatorial Currents. Wind Driven Circulation.

Further Reading

Dodimead AJ, Favorite JF and Hirano T (1963) Review of oceanography of the subarctic Pacific region. *Bulletin of International North Pacific Fisheries Commission* 13: 1–195.

Kawabe M (1995) Variations of current path, velocity, and volume transport of the Kuroshio in relation with the large meander. *Journal of Physical Oceanography* 25: 3103–3117.

Kawai H (1972) Hydrography of the Kuroshio Extension. In: Stommel H and Yoshida K (eds) *Kuroshio – Its Physical Aspects*, pp. 235–354. Tokyo: University of Tokyo Press.

Mizuno K and White WB (1983) Annual and interannual variability in the Kuroshio Current system. *Journal of Physical Oceanography* 13: 1847–1867.

Nitani H (1972) Beginning of the Kuroshio. In: Stommel H and Yoshida K (eds) *Kuroshio – Its Physical Aspects*, pp. 129–163. Tokyo: University of Tokyo Press.

Pickard GL and Emery WJ (1990) *Descriptive Physical Oceanography: An Introduction*, *5th edn.* Oxford: Pergamon Press.

Shoji D (1972) Time variation of the Kuroshio south of Japan. In: Stommel H and Yoshida K (eds) *Kuroshio – Its Physical Aspects*, pp. 217–234. Tokyo: University of Tokyo Press.

Taft BA (1972) Characteristics of the flow of the Kuroshio south of Japan. In: Stommel H and Yoshida K (eds) *Kuroshio – Its Physical Aspects*, pp. 165–216. Tokyo: University of Tokyo Press.

Tomczak M and Godfrey JS (1994) *Regional Oceanography: An Introduction*. Oxford: Pergamon Press.